Heritage Science

RESEARCH Open Access

Combined studies on glazed ceramic bodies from the Middle and Neo-Elamite periods (1500–539 BCE)

Ali Aarab[1,2,3*], Laurent Cormier[2], Bahman Firoozmandi[3] and Martine Gérard[2]

Abstract

The Elamites have assigned specialized names for different types of ceramics, signaling a specialized approach to ceramic production during the Middle and Neo-Elamite periods. They were pioneers in the use of glazed ceramics on the Iranian Plateau. This investigation focuses on the examination of 29 samples of glazed ceramic bodies originating from the Middle-Elamite (~ 1500–1100 BCE) and Neo-Elamite periods (~ 1100–539 BCE). The objective of this analysis, centered on the earliest instances of glazed ceramic bodies in Iran, is to obtain a comparative examination of the ceramic bodies. Such an approach can be useful for understanding the diverse production techniques used by Elamites in the Middle-Elamite and Neo-Elamite periods. To achieve this purpose, X-ray diffraction and petrography was used to determine the mineralogical characteristics of the ceramic bodies. Further insight into the chemical analysis of the samples was obtained through Electron Probe Micro-Analysis. The experimental data allowed the classification of the samples into four distinct groups. Particularly noteworthy in this categorization is the diversity observed in the Neo-Elamite samples. This diversity of Neo-Elamite ceramic bodies can be attributed to two primary factors. Firstly, the Neo-Elamite period witnessed a more varied array of techniques for producing glazed ceramic bodies compared to the Middle-Elamite period. Unlike the Middle-Elamite glazed ceramics, which were solely utilized for architectural decoration (glazed bricks) and were locally produced, the Neo-Elamite period marked the first instance of glazed ceramic vessels being used in the southwest of Iranian plateau, leading to a higher technological diversity. Secondly, the frequency of trade and importation of glazed ceramics from other regions to the southwest of Iran was notably higher during the Neo-Elamite period compared to the Middle-Elamite one. A notable distinction emerges in the Middle-Elam period, where exclusively quartz-based ceramic bodies were referenced, setting it apart from other sample types.

Keywords Middle-Elamite, Neo-Elamite, Glazed bricks, Glazed pottery, Firing temperature

*Correspondence:
Ali Aarab
ali.aarab@ucas.ac.cn
Full list of author information is available at the end of the article

Introduction

The earliest evidence of glazing on ceramic artifacts in the Iranian Plateau dates back from to the fourteenth century BCE, found at the archaeological site of Haft Tappeh. Although glazed ceramics at this site have received less attention, archeological excavations have unearthed evidence supporting the use of glazes on ceramic surfaces [1]. While the extent of their applications appears somewhat limited based on current findings, the discovery of spools at the Haft Tappeh site [2], associated with Tepti Ahar, an Elamite king from the fifteenth century BCE, can be regarded as early instances of glazed objects within the Elamite period. However, even at Haft Tappeh, examples of glazed bricks have not been identified and only small glazed objects have been recovered. Therefore, the advent of glazed brick usage is thought to be linked to the Chogha Zanbil site (~ thirteenth century BCE). While comprehensive studies have been conducted on glazed ceramics from the Elamite period [3–5], it should be noted that, to date, certain examples of Neo-Elamite glazed ceramics, like those from the Jubaji site, have not undergone thorough investigation. The earliest evidence of ceramic glazing among Mesopotamian civilizations dates back to the middle of the second millennium BCE [6]. Therefore, the Elamite civilization (during the Middle-Elamite period) can be considered one of the first civilizations in the Near East to use glazed ceramics for architectural decorations [7]. The use of glazed ceramics in the Haft Tappeh site, dating back to the middle of the second millennium BCE, has been reported in southwestern Iran [1]. Given that Mesopotamia and Egypt can be considered among the earliest regions where glass-making began, with dates close to the middle of the second millennium BCE [8], the discovery of glazed ceramics in the middle of the second millennium BCE at the Haft Tappeh site, related to the Middle-Elamite period, could have been influenced by trade connections with Mesopotamia. This highlights the significant importance of Middle-Elamite glazed ceramics in Iran.

Extensive studies have also been carried out on glazed ceramics at the Susa site [4]. However, one of the challenges encountered in studying glazed ceramics at the Susa site lies in the issue of stratigraphy, which complicates the dating of some glazed ceramics. For example, determining the precise dates of glazed bricks from the Neo-Elamite (~ 1100–539 BCE) and Achaemenid (~ 550–330 BCE) period in Susa can be quite complex at times [9].

Analyzing glazed ceramics spanning from the Middle to the Neo-Elamite periods holds paramount significance for unraveling insights into material origins, production techniques and the dynamics of economic and cultural exchanges. Notably, there has been a scarcity of analyses conducted on unglazed ceramics of Elamite origin [10]. It should be noted that the use of glazed ceramics during the Middle-Elamite period was not limited to the southwestern region of the Iranian Plateau; evidence of glazed ceramics has also been found in the Tall-e Malyan region in southern Iran [11]. However, this study primarily focuses on the technological evolution of glazed ceramics from the Middle-Elamite to Neo-Elamite periods and from architectural glazed ceramics to glazed wares, with a specific emphasis on the southwestern region of Iran. A recent investigation was focused on glazed ceramic bodies originating from the Middle-Elamite to the Achaemenid periods [3]. The findings of this study indicate that the ceramic bodies were produced from calcareous clays abundant in fragments of limestone, flint, grog, and organic temper. The authors mentioned that the glazing process involved the application to biscuit-fired bodies rather than dried green bodies.

One valuable source for gaining insights into the raw materials and manufacturing processes of ceramics from the Elamite period lies in the surviving written records. The Elamite language contains distinct terms for describing baked and mud ceramic bodies, primarily associated with the introduction of mudbricks, baked bricks, and glazed bricks. Information on these words is provided in Table S1 [12], emphasizing the linguistic nuances in referring to Elamite bricks. The striking aspect about the frequency and diversity of terms employed for ceramic bodies describing Elamite bricks underscores the varied and specialized techniques employed in ceramic production during that epoch. Notably, in the twelfth century BCE, King Shutruk Nahunte I (~ 1184–1150 BCE) claimed credit for pioneering a novel brick processing technique known as *akti*. This method involved highly siliceous bodies designed to imitate stone. Another example of linguistic diversity during the Middle-Elamite period, specifically during the Untash Napirisha reign, is the use of the term *mush* to characterize glazed ceramic [13, 14]. Siliceous ceramic bodies from the Elamite period have been introduced and studied as an important invention [4]. However, these specialized terms, reflective of technological innovations in the Middle and Neo-Elamite periods, must be complemented and compared through archaeometric studies on glazed ceramics. Such studies are instrumental in identifying raw materials and enhancing our understanding of the relationships between elaboration techniques and firing conditions employed during these historical periods. Furthermore, in this study, efforts have been made to explore the technological advancements documented in Elamite texts by analyzing glazed ceramic compositions. Essentially, the aim is to trace the evolution of the new type of ceramics

featuring a siliceous body from its inception to the Neo-Elamite period, while identifying its key distinctions from earlier ceramic types. Then, the aim of this study was to conduct a comprehensive comparison of the mineralogy and microstructure of ceramic bodies derived from glazed samples belonging to both the Middle-Elamite and Neo-Elamite periods in southwest Iran. This approach, utilizing a multianalytical methodology, serves to document the materials and techniques used in the creation of these objects. In other words, this research offers the initial opportunity to delve into the technology of crafting glazed ceramic bodies in southwest Iran, particularly in the Khuzestan province, with a focus on sites like Haft Tappeh, Chogha Zanbil, and Jubaji. Initially, glazed ceramic bodies during the Middle-Elamite period were solely used for architectural decorations [15]. However, during the Neo-Elamite period, glazed ceramic bodies in vessel form began to emerge [16]. Hence, studying the technological shift in glazed ceramic bodies in southwest Iran holds significant importance. Regarding the study sites in the current research, it is also worth mentioning that two sites, Haft Tappeh and Chogha Zanbil can be considered from the Middle-Elamite cities, with Haft Tappeh referred to as the ancient city of Kabnak and Chogha Zanbil known as the city of Dur-Untaš [17, 18]. The Neo-Elamite site, Jubaji, is actually a cemetery dating back to the Neo-Elamite period and was not a settlement [19].

Materials

In the investigation of glazed ceramic bodies related to the Elamite world, 29 samples were selected from three distinct sites—Haft Tappeh, Chogha Zanbil, and Jubaji—in Khuzestan Province of southwestern Iran (Fig. 1a). The chosen samples are related to the periods of Middle-Elam (Haft Tappeh and Chogha Zanbil) and Neo-Elam (Jubaji). Table 1 provides details regarding the approximate periods of the examined ceramics, along with information on the nature and number of fragments. All the glazed ceramic bodies were obtained from archaeological excavations conducted in the Khuzestan province of Iran. The samples, including glazed bricks and wares, from the Chogha Zanbil ziggurat were collected during archaeological excavations supervised by Ghirshman [20]. Neo-Elamite glazes originated from the Jubaji site excavation [19]. The Jubaji specimens were exclusively obtained from Elamite tombs interred within a mortuary structure. Two samples from Haft Tappeh are spools discovered in the Middle-Elamite layer of this site (Fig. 1b). These objects were obtained from archaeological excavations directed by Negahban [1]. Among the glazed ceramics from Haft Tappeh, these samples are particularly noteworthy, representing early instances of ceramic glazes in Iran. Although Susa is another Elamite site known for glazed ceramics, it was excluded from the current study. Abbreviations for ancient sites were employed throughout this study. Consequently, "CZT" serves as the abbreviation for Chogha Zanbil, "HT" as the abbreviation for Haft Tappeh, and "J" as the abbreviation for Jubaji.

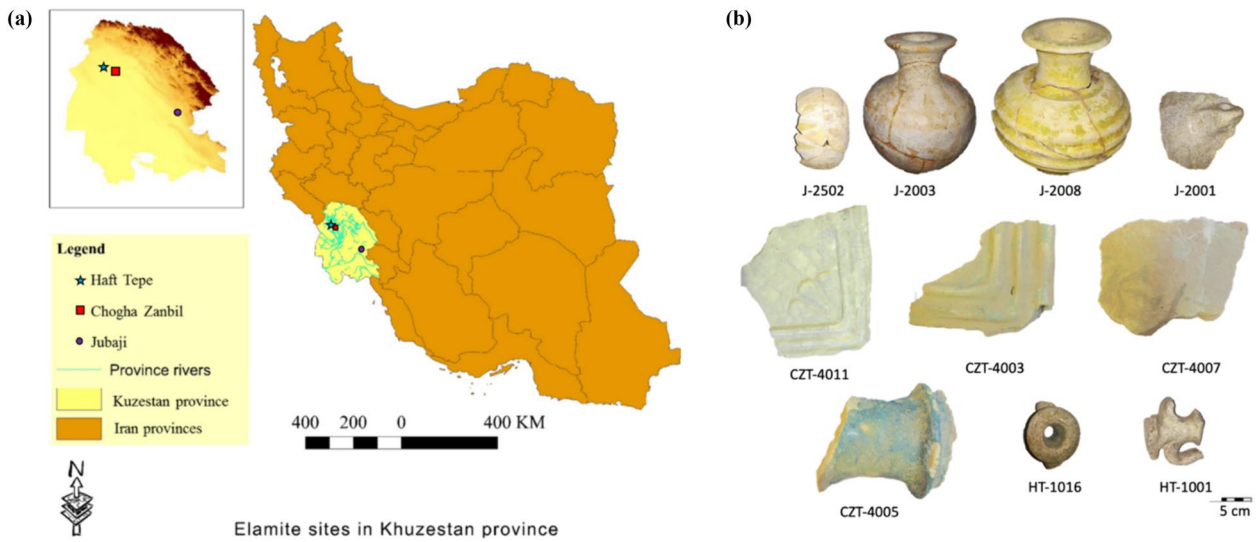

Fig. 1 **a** Geographical location of the studied Elamite sites in southwestern Iran. **b** Photographs of representative glazed objects from both the Middle- and Neo-Elamite periods

Table 1 Fragments of glazed bodies studied in the present study

Number	Sample	Possible use	Glaze color	Period	Characterization
1	CZT-4007	Building decoration	White	Middle-Elam (~1300 BCE)	XRD
2	CZT-4012	Building decoration	Blue/White	Middle-Elam (~1300 BCE)	XRD, EPMA
3	CZT-4011	Building decoration	White	Middle-Elam (~1300 BCE)	XRD, Petrography, EPMA
4	CZT-4005	Building decoration	Blue	Middle-Elam (~1300 BCE)	XRD, EPMA
5	CZT-4013	Building decoration	White/Black	Middle-Elam (~1300 BCE)	XRD, Petrography, EPMA
6	CZT-4001	Building decoration	White/Blue	Middle-Elam (~1300 BCE)	XRD, EPMA
7	CZT-4004	Building decoration	Blue	Middle-Elam (~1300 BCE)	XRD, Petrography, EPMA
8	CZT-4002	Building decoration	White	Middle-Elam (~1300 BCE)	XRD, EPMA
9	CZT-4010	Building decoration	Blue	Middle-Elam (~1300 BCE)	XRD, EPMA
10	CZT-4006	Building decoration	White/Blue	Middle-Elam (~1300 BCE)	XRD, Petrography, EPMA
11	CZT-4009	Building decoration	Blue/Green	Middle-Elam (~1300 BCE)	XRD, EPMA
12	CZT-4014	Building decoration	Blue	Middle-Elam (~1300 BCE)	XRD, EPMA
13	CZT-4008	Building decoration	Blue/White	Middle-Elam (~1300 BCE)	XRD
14	HT-1016	Spool (knob)	White/Blue	Middle-Elam (~1500 BCE)	XRD, Petrography, EPMA
15	HT-1001	Spool (knob)	White	Middle-Elam (~1500 BCE)	XRD, Petrography, EPMA
16	J-2008	Pottery	Green/Yellow	Neo-Elam (~539 BCE)	XRD
17	J-2505	Pottery	Yellow/White	Neo-Elam (539 BCE)	XRD, EPMA
18	J-7009	Pottery	Green	Neo-Elam (539 BCE)	XRD, Petrography, EPMA
19	J-2009	Pottery	Green	Neo-Elam (539 BCE)	XRD, Petrography, EPMA
20	J-2001	Pottery	White	Neo-Elam (539 BCE)	XRD, EPMA
21	J-7008	Pottery	Blue	Neo-Elam (539 BCE)	XRD, EPMA
22	J-2501	Pottery	Green	Neo-Elam (539 BCE)	XRD, EPMA
23	J-2004	Pottery	Yellow	Neo-Elam (~539 BCE)	XRD, EPMA
24	J-2503	Pottery	White/Blue	Neo-Elam (~539 BCE)	XRD, EPMA
25	J-2007	Pottery	Green	Neo-Elam (~539 BCE)	XRD, EPMA
26	J-2502	Pottery	White/Yellow	Neo-Elam (~539 BCE)	XRD, EPMA
27	J-2006	Pottery	Blue	Neo-Elam (~539 BCE)	XRD, EPMA
28	J-2002	Pottery	Blue/White	Neo-Elam (~539 BCE)	XRD
29	J-2003	Pottery	Yellow/White	Neo-Elam (~539 BCE)	XRD, Petrography, EPMA

CZT, J and HT indicate samples originating from Chogha Zanbil, Jubaji and Haft Tappeh, respectively

Methods

X-ray powder diffraction

X-ray powder diffraction (XRPD) measurements were performed on a PANalytical X'Pert PRO (Amelo, Netherlands) diffractometer. Co Kα radiation was used at 45 kV and 40 mA. Diffraction patterns were collected with an X-Celerator detector over an angular range of $5° \leq 2\theta \leq 100°$, using a step of 0.0167° (2θ) and a scanning rate of 3 s/step. For all samples, the zones analyzed by XRPD were chosen from the central section of the ceramics and finely crushed into powder. Diffractogram analysis was performed using X-Pert High Score Plus software (Panalytical) to identify crystalline phases based on peak locations and intensities using ICDD patterns. The data acquired from the X-ray powder diffraction analyses were subjected to a multivariate statistical procedure known as principal component analysis (PCA). This analytical technique is being used as a valuable tool for grouping samples and emphasizing relationships among different fragments [21]. PCA was executed using HighScore Plus software.

Thin-section petrography

To characterize the microstructures of the Middle- and Neo-Elamite fragments, a petrographic study was carried out on 12 thin sections. Due to limitations in sampling Elamite glazed ceramics, the petrographic study was restricted to 12 samples, which were selected based on two groups of potteries and bricks. The ceramic fragments were prepared by impregnation in epoxy and subsequent polishing to a thickness of 30 µm. Optical observations were carried out using a polarizing microscope (Olympus) that used transmitted plane-polarized (PPL) or cross-polarized (XP) light. For quality control in thin section preparation, quartz served as a reference material due to its abundance and well-known optical

properties. Quartz, being readily available, ensured that the sample material achieved an appropriate thickness, making it an excellent reference material for ceramic studies. The thin sections were examined and described using a polarizing microscope following established criteria developed in previous studies [22]. This approach facilitated a comprehensive characterization of the microstructures present in the ceramic fragments.

Ceramic petrography integrates methodology from sedimentology and sedimentary petrography, such as the description of particle shape and texture. Drawing upon principles from the microscopic study of soils, ceramic petrography provides a comprehensive description of the nature of the matrix and the presence of pores or 'voids' within ceramic artifacts [23].

Scanning electron microscopy

Scanning electron microscopy (SEM) analysis was used to observe the microstructure of the ceramic bodies, using a Zeiss Ultra55 instrument equipped with a field emission gun. The analysis specifically targeted samples exhibiting a distinct structure as identified through the preliminary petrographic study. SEM micrographs are particularly valuable for examining pottery firing temperatures and structure characteristics [24, 25]. Energy dispersive X-ray spectroscopy (EDXS) microanalysis has also been widely applied for identifying constituents in ancient bodies and glazes offering qualitative and quantitative insights into their chemical compositions [21]. EDXS point analysis was performed using an EDXS QUANTAX system equipped with a silicon drift detector (XFlash 4010; Bruker).

Electron probe micro analysis

Electron probe microanalysis (EPMA) was used to investigate the chemical composition of the 20 selected ceramic bodies, using a CAMECA SX5 electron microprobe equipped with a wavelength-dispersive spectrometer (WDS) at the Camparis Center (Sorbonne Université, Paris, France). Two distinct operating conditions were applied: 15 keV accelerating voltage and 10 nA beam current for major elements (Na, Mg, Al, P, K, Ca, Ti, and Fe: Kα) and 25 keV–299 nA for minor elements (V, Sr, Ni, Cr, Co, Zn, and Ba). The beam was focused to a spot size of 40 µm for point analysis, and a short counting time was employed to mitigate alkali migration. For calibration purposes, the standards used included albite, diopside, orthoclase, apatite, MnTi, Fe_2O_3, PbS, $BaSO_4$, FeS_2, Cr_2O_3, NiO, ZnS, $SrSiO_3$, $ZrSiO_4$ and metals (V, Co, Cu). The samples were impregnated in epoxy resin, polished and then carbon-coated. Ten points were measured on each ceramic body for analysis, allowing for the determination of the average chemical composition.

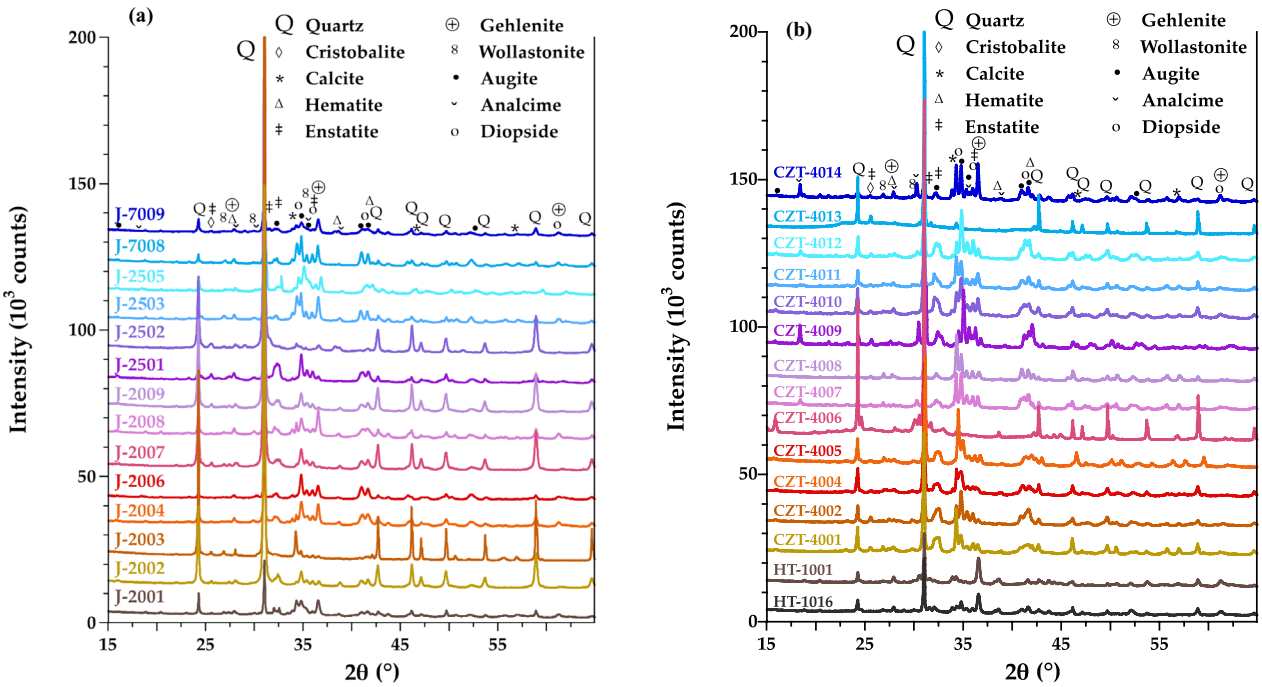

Fig. 2 **a** XRPD diffractograms obtained for ceramic bodies of the Neo-Elamite samples from Jubaji (pottery samples) showing the main crystalline phases. **b** XRPD diffractograms obtained on ceramic bodies of the Middle-Elamite samples from Chogha Zanbil and Haft Tappeh (building decorations) with the main crystalline phases

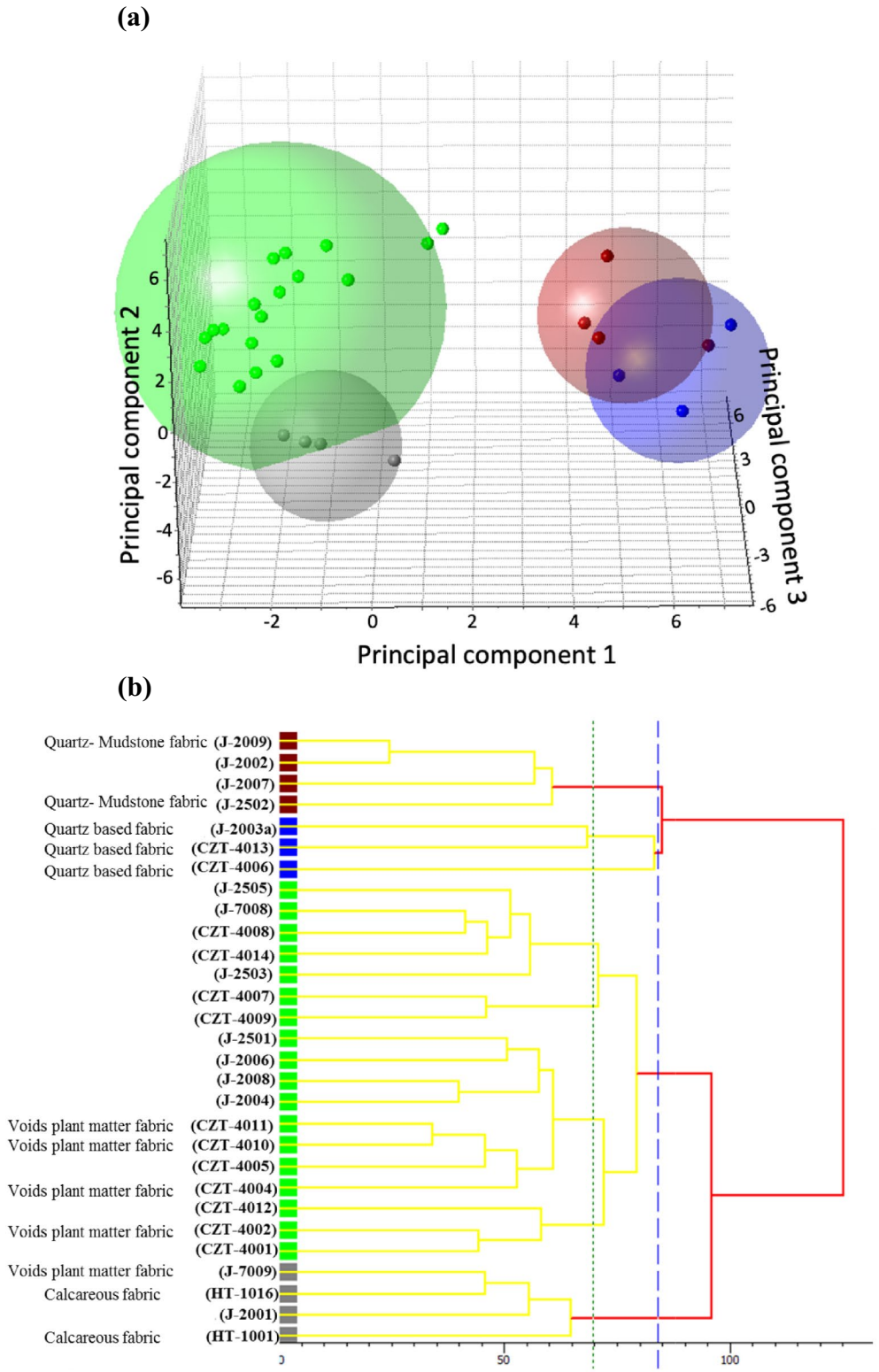

Fig. 3 **a** PCA plot of ceramic bodies (73.87% var) based on XRPD diffractograms, **b** Dendrogram of PCA results derived from XRPD diffractograms

Results

Crystalline phase composition

XRPD analysis was conducted on 29 glazed ceramics to elucidate the mineralogy of the ceramic bodies. A search and match algorithm, based on the 2θ positions within the diffraction patterns (Fig. 2), was used to determine the crystalline phases present. The predominant crystalline phases identified in the ceramic bodies encompassed quartz, diopside, enstatite, calcite, augite, albite, and gehlenite. These phases are indicative of either raw materials (quartz and plagioclase such as albite) or secondary minerals formed during high temperature firing (augite, diopside, gehlenite, anorthite, enstatite) or during the weathering process occurring after burial of the samples [26].

A principal component analysis (PCA) was performed on the XRPD patterns of the studied samples (Fig. 3). PCA, when applied to XRPD results obtained from ceramic bodies, enhances the understanding of sample classification. In this method, the original *n*-dimensional hyperspace, defined by the samples and XRPD patterns, is transformed into a new Principal Component (PC) space with reduced dimensionality. The samples are then projected in this newly defined PC space, where the coordinate values, known as scores, facilitate a more refined categorization of the samples [27]. Based on the PCA diagram of the ceramic bodies from Middle- and Neo-Elamite, the samples can be differentiated into four discernible groups. The PCA results are further presented in the form of a dendrogram, generated through cluster analysis using HighScore software, with the sample names depicted in Fig. 3b. This dendrogram provides a clearer understanding of the relationships between the samples, offering valuable insights into the classification and similarities among the studied ceramic bodies.

In Fig. 3a, a distinct group marked in blue comprises three samples (CZT-4013, CZT-4006 and J-2003). The corresponding diffractograms (Figure S1) reveal a substantial presence of quartz, along with calcite. An appreciable amorphous phase is also observed, indicated by a significant bump between 20 and 35°. The second group, highlighted in red in Fig. 3a, closely aligns with the previous group and consists of four samples (J-2502, J-2009, J-2007 and J-2002) exclusively from the Neo-Elamite period. The diffractograms (Figure S2) for this group indicate the presence of quartz, augite, gehlenite, wollastonite, diopside and calcite. The largest group, denoted in green in Fig. 3a, includes eleven samples from the Middle-Elam and seven samples from the Neo-Elam. The diffractograms for this group (Figure S3) are complex with the presence of quartz, though in a lesser amount compared to other groups. Various phases such as calcite, augite, gehlenite, wollastonite, diopside and enstatite can be detected. Analcime is also observed in some samples, with a characteristic peak at $2\theta = 18.41°$. The last group, marked in gray in Fig. 3a, consists of four samples (J-7009, J2001, HT-1016 and HT-1001) and is closer to the green group. The diffractograms (Figure S4) for this group are dominated by quartz with minority phases such as gehlenite, calcite and augite, akin to Group 3. In all groups, the presence of iron oxide (hematite) was detected, and the size of the crystals suggests a potential role in the observed yellow–orange coloration of some ceramic bodies.

Microstructure

According to the petrographic analysis, all samples were classified into four distinct types based on their crystalline contents: quartz-based (siliceous), quartz-mudstone, void-plant matter, and calcareous (Fig. 4).

Quartz-based (siliceous) type

This group encompasses three samples (CZT-4006, CZT-4013, and J-2003 in Fig. 4a-c) and corresponds to group 1-blue, as identified through XRPD analysis. The mineralogy of this group is primarily characterized by the presence of quartz grains. The size, angular shape, and distribution of the quartz crystals differ between these ceramics and other samples. Specifically, the quartz grains in CZT-4006 are larger than those in the other samples, and the quartz grains in J-2003 and CZT-4006 exhibit sharper angles compared to those in CZT-4013. Additionally, needle-shaped crystals are observed in this group (Fig. 4j), potentially indicating a carbonate type. If confirmed, this fabric closely resembles the sandstone fabrics found in ancient ceramics [28]. Due to these characteristics, this group of ceramics was classified as having poorly sorted angular textures. Quartz-based (siliceous) bodies were used in Elam as a local architectural decoration, representing a distinctive feature of Elamite architecture until the end of the Neo-Elamite period (c. 1000–539 BCE) [29]. The term "siliceous" or similar descriptors, such as "quartz-based", include a broad spectrum of ceramic bodies from the Elamite period [14, 30]. This fabric is likely associated with *akti* a term attributed to Shutruk Nahunte I, who considered himself its inventor.

Quartz-mudstone tempered type

This group comprises two samples (J-2009 and J-2502), both dating to the Neo-Elamite period, and falling within group 2-red as identified by XRPD analysis. These samples are characterized by angular mudstone fragments and quartz as reference (Fig. 4d). In this fabric group, the proportion of quartz crystals is lower than that in fabric "a" but higher compared to that in fabric "c" and

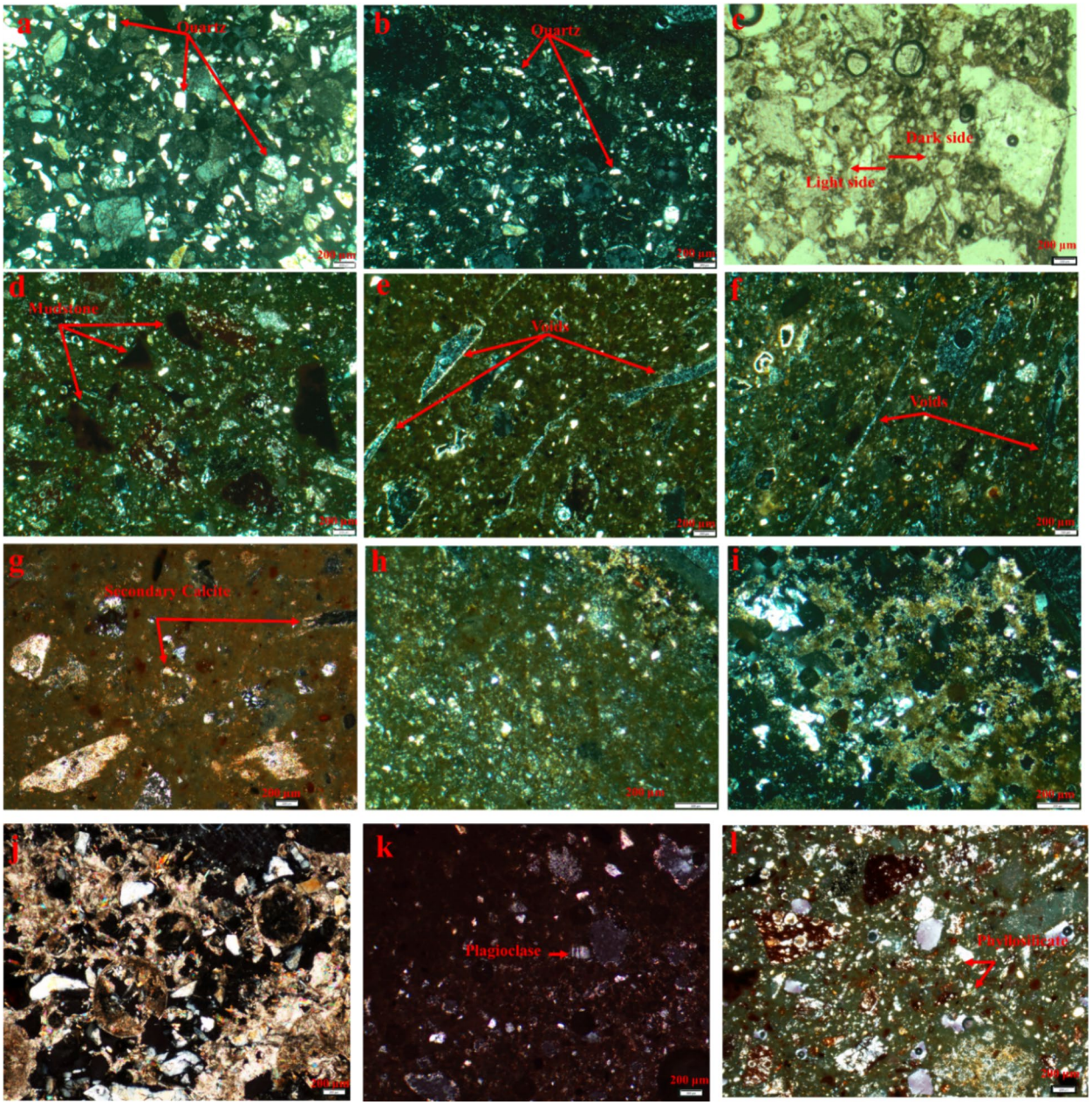

Fig. 4 Photomicrographs of thin sections (scale 200 µm) showing different types of ceramic bodies. **a** Quartz base fabric, CZT-4006, XPL; **b** Quartz base fabric, CZT-4013, cross-polarized (XPL); **c** Quartz base fabric, J-2003 [dark side] and [light side], plane-polarized (PPL); **d** Quartz-Mudstone fabric, J-2009, XPL; **e** Void plant matter fabric, CZT-4004, XPL; **f** Plant matter fabric, CZT-4011, XPL; **g** Secondary calcite formation in the voids of void plant matter fabric, J-7009, PPL; **h** Calcareous fabric and carbonate groundmass, HT-1001, XPL; **i** Calcareous fabric and carbonate groundmass, HT-1016, XPL; **j** Carbonate needles, Quartz base fabric, CZT-4006, XPL; **k** Plagioclase, Void plant matter fabric, CZT-4011, XPL; **l** Phyllosilicates, Quartz- Mudstone fabric, J-2009, XPL

"d". Notably, phyllosilicate minerals are observed in this group of samples (Fig. 4l), and the presence of phyllosilicate minerals in pottery is often indicative of the firing temperature [31]. Therefore, due to the presence of quartz and phyllosilicate minerals, it is anticipated that the chemical composition of these samples contains a substantial amount of silica oxide.

Void-plant matter type

A significant part of the Chogha Zanbil samples falls into this group, exemplified by samples CZT-4004 and

CZT-4011 (Fig. 4e, f). These samples are also affiliated with group 3-green, as indicated by XRPD analysis. Petrographic images reveal the frequent use of tempering agents, specifically organic matter, which, over time, decayed or burned out. In this group, the presence of characteristic voids is indicative of tempering with plant matter. Organic inclusions sometimes display preserved vegetal microstructures (plant remains), and burnt traces of this organic matter are observed in the ceramic. Numerous grains are composed of opaque black matter featuring microcracks and are hollow in the middle (carbonaceous residues) [32]. The high quantities of organic matter in the Chogha Zanbil samples may suggest intentional addition to the clay by potters at this site. The organic materials incorporated into the pottery were lost during the firing process, leaving behind empty space. Petrographic analysis of the samples from this fabric reveals that the voids created during firing provide suitable conditions for the formation of secondary calcite (Fig. 4g). Therefore, the detected amount of calcium oxide in samples of this fabric is not linked to the initial conditions of pottery preparation and firing but rather to subsequent transformations during firing.

In general, primary calcite is associated with rather low firing temperatures (less than 750 °C), preventing calcite from undergoing decarbonatation. However, the size of the grains and the firing atmosphere strongly influence the stability of calcite, and occurrences can also be observed when firing temperatures reach 800 °C. Secondary calcite, formed after ceramic firing, can take various forms, including reformed (recarbonated) calcite, precipitated calcite, or calcite resulting from alteration [33]. The origin of these secondary calcite crystals is diverse, and several pathways for crystallization have been proposed in literature [34]:

1. Filtration of calcareous aqueous solutions during burial conditions, followed by the recrystallization of secondary calcite,
2. Secondary calcite formed by the decomposition of gehlenite under post-burial chemical leaching,
3. Recarbonatation of portlandite [$Ca(OH)_2$] generated by the hydration of unreacted lime (CaO).

Furthermore, in this fabric, a small amount of plagioclase can be identified among the samples (Fig. 4k). Consequently, it is expected that the samples in this fabric contain a relatively high amount of aluminum oxide.

Calcareous type

The two Haft Tappeh samples (HT-1016, HT-1001) were included in this group due to the yellow groundmass of these samples. These samples align with group4-red according to XRPD analysis. Some samples of the void-plant matter type are similar in groundmass to the two samples included in the calcareous type. The groundmass of this type (Fig. 4h, i) varies from light brown/yellow (plane polarized, × 400) to yellowish/brown (cross polarized, × 400). The presence of carbonates in ancient pottery may influence the yellow color in the groundmass of pottery containing iron [35]. The yellow color indicates a higher concentration of calcium in these samples compared to other. However, it is important to note that calcium can be abundant in samples where plant matter serves as a temper, potentially explaining the formation of secondary calcite in the voids of plant matter. Moreover, the intensity of yellow in the groundmass of calcareous type samples surpasses that in void plant matter type samples, suggesting the presence of additional calcium in their texture.

Chemical composition

EPMA was performed on the samples to investigate their chemical compositions, and the results are reported in Tables S2 and S3. Given the constraints associated with sampling Elamite specimens, a total of 25 samples were selected for EPMA analysis. Consequently, samples CZT-4007, CZT-4008, J-2002, and J-2008 were excluded from the analysis due to their limited quantity. To distinguish between ceramic bodies from the Elamite periods, the results were plotted in a ternary diagram SiO_2-Al_2O_3-(MgO + CaO) (Fig. 5a). The sample distributions align closely with previous studies on Haft Tappeh and Chogha Zanbil samples [36], demonstrating consistent trend with most points extending along almost constant Al_2O_3 contents. The majority of samples can be classified as calcium-rich ceramics [10, 37]. A notable outcome is the high SiO_2 content in seven samples (J-2002, J-2003, J-2502, J-2009, J2007, CZT-4006, and CZT-4013), positioning them in the SiO_2-rich domain. This is interesting as these seven samples correspond to the siliceous fabric and the Quartz-Mudstone tempered fabric, as identified in the petrographic analysis above. The high SiO_2 content is consistent with the prevalence of quartz in these samples, corresponding to Group 1-blue and Group 2-red in XRPD analysis. Essentially, these seven samples are located beyond or close to the quartz/anorthite line, indicative of the noncalcareous field [37]. Examining the proportion of calcium in the samples, the percentages of CaO in samples CZT-4006, J-2003, and CZT-4013 (siliceous fabric based on petrography) are less than 6 wt%. Interestingly, according to the XRPD diffractograms, the amount of the amorphous phase in these samples is greater than that in the other samples. This likely indicates high melting temperatures, which

are needed for sintering such highly siliceous materials. Conversely, in ceramics made from calcareous clays, the development of vitrification is inhibited by the formation of crystalline phases at high melting temperatures, such as calcium aluminosilicates (anorthite, gehlenite) and calcium/magnesium silicates (wollastonite, diopside) [24].

Moreover, in the SiO_2-Al_2O_3-(CaO + MgO) ternary diagram, the diopside/wollastonite-gehlenite-anorthite triangle is related to highly calcium-rich samples. Three samples (HT-1001, HT-1016, and J-2001) fall within this region of the ternary diagram (Fig. 5a) and are primarily aligned with the group 4-Gy identified by XRPD analysis. According to the petrographic analysis, sample HT-1001 contains a significant number of limestone fragments (the first group of calcareous types). The EPMA results and SiO_2-Al_2O_3-(CaO + MgO) ternary diagram thus corroborate the petrographic findings. A salient feature that emerges from the ternary diagram is the considerable scattering of samples along the SiO_2-(CaO + MgO) line. This suggests that the raw clayey matrices have relatively constant Al_2O_3 contents and the differences in chemical composition mainly arise from variations in the SiO_2/(CaO + MgO) ratios within the matrices [26].

Discussion

The predominant component observed in the Elamite glazed ceramics was quartz. Diopside and enstatite, belonging to the pyroxene group, were found in increasing amounts above a temperature of 840 °C [38]. Diopside drastically appears at 950 °C [39], and its main diffraction peaks intensifies significantly at temperatures higher than 950 °C [40]. The presence of diopside in ceramic bodies may be associated with carbonates (possible dolomite) in the clayey material. The reaction between carbonates and

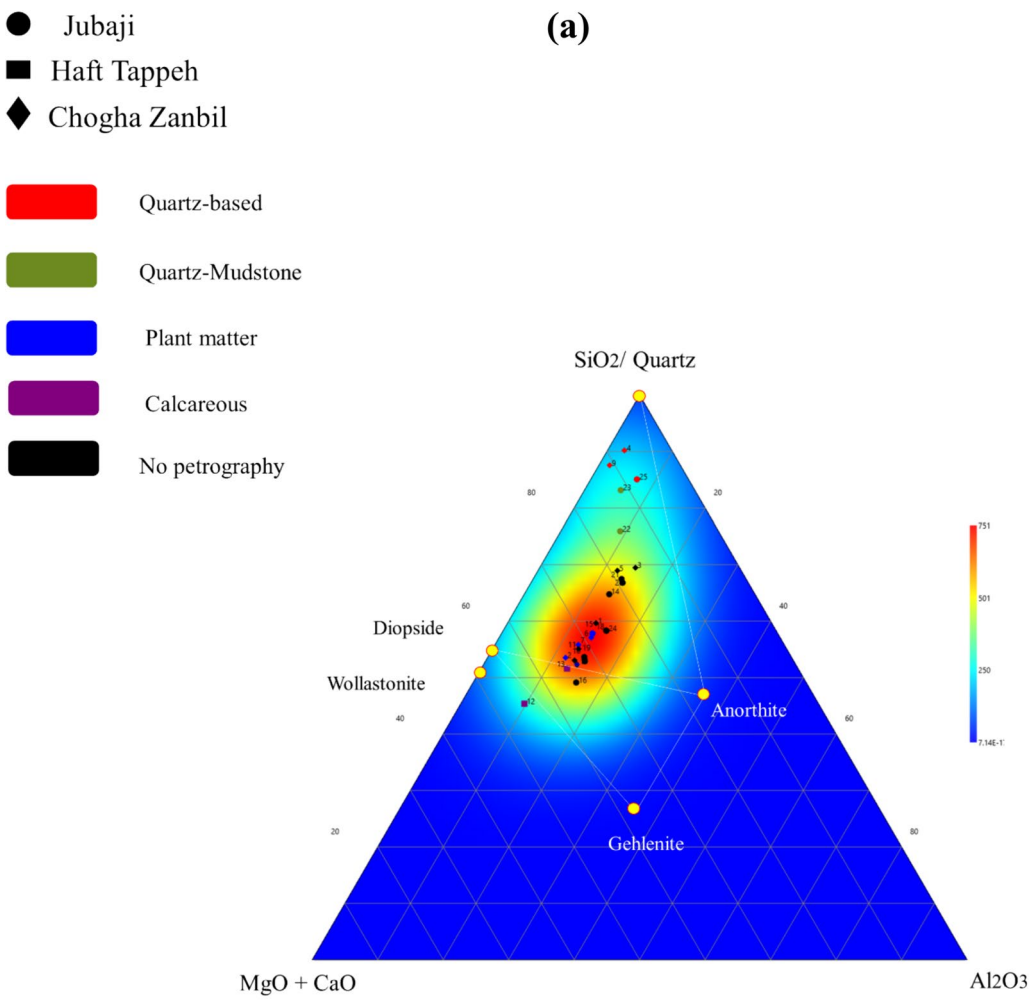

Fig. 5 **a** Bulk chemical composition (wt%) of the different analyzed ceramic bodies plotted in the ternary SiO_2-Al_2O_3-(CaO + MgO). The intensity represents the density of the samples identified in different regions on the ternary. **b** X-ray diffraction pattern of mordenite in sample CZT-4006. **c** Quartz cores with cristobalite edges in Neo-Elamite samples, based on the wares of the Song dynasty [51]

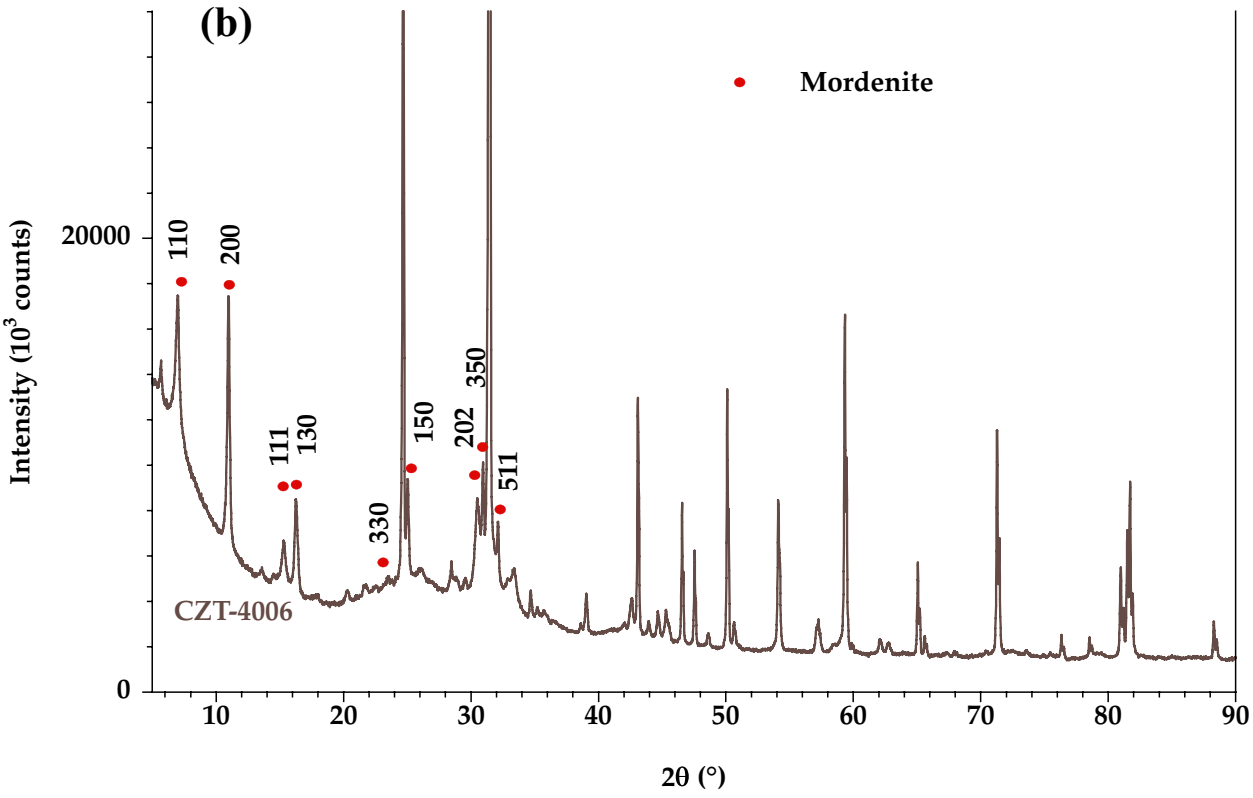

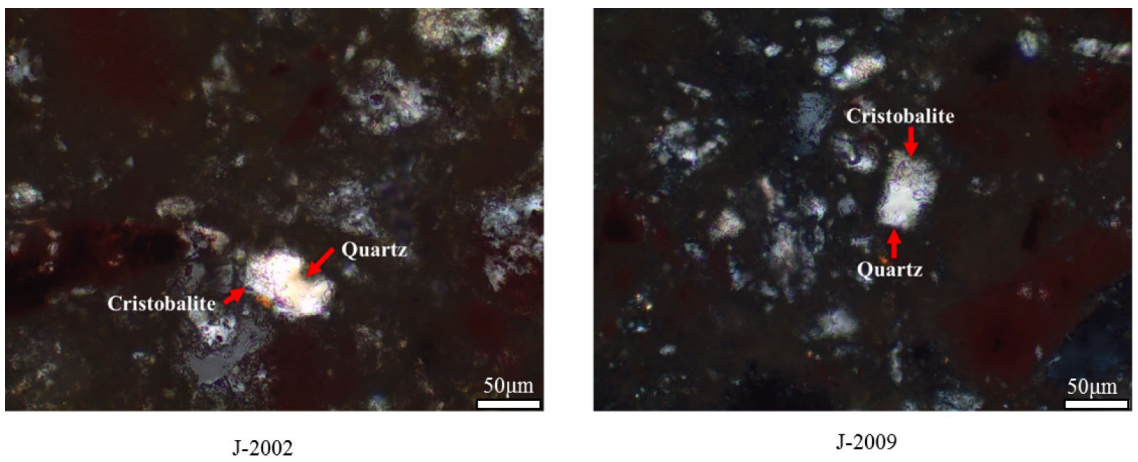

Fig. 5 continued

quartz can lead to the formation of diopside at temperatures around 900 °C [21]. Additionally, crystalline structures resembling enstatite can formed from Mg-silicates, such as talc, or clay minerals, such as Mg-rich smectite, through a topotactic phase transformation at temperatures above 700 °C to 1000 °C [41]. Gehlenite begins to crystallize above 850 °C, as evident from the XRPD patterns [42]. When ceramics are fired at temperatures exceeding 1000 °C or for extended periods at the maximum temperature, the gehlenite content is expected to decrease as it reacts with residual quartz to give anorthite and wollastonite [34]. Moreover, åkermanite remains

stable between 744 °C and 875 °C [38]. Javanshah suggested that the presence of albite in ancient ceramics indicates firing at approximately 900 °C [43]. However, albite, like quartz and feldspars (orthoclase and microcline), can be present at all temperatures as it are resistant even at high temperatures [44]. Additionally, albite undergoes a triclinic-to-monoclinic phase transition near 980 °C, leading to the formation of "high albite", which has a disordered Al-Si arrangement (in contrast to "low albite") [45]. The presence of hematite in most ceramic bodies is indicative of an oxidative firing atmosphere in the kiln and may result from the use of iron-rich clay as a raw material [46].

The mineral phases identified in the XRPD analysis suggest varying firing temperatures for the ceramic bodies. Generally, the presence of secondary minerals is a signature of a firing temperature between 850 °C and 1000 °C. However, the lack of significant calcite in group 1-blue and group 2-red indicates that the firing temperature for these materials exceeds that in group 3-green and group 4-Gy. This is further confirmed by the considerable amount of amorphous phase observed in the XRPD patterns of the samples in groups 1-blue. High-temperature mineral phases such as diopside have been identified in these samples, but some minerals stable at lower temperatures, such as åkermanite and calcite, have not been detected. Moreover, the XRPD patterns of samples CZT-4006 and CZT-4013 are completely different from each other due to the presence of an amorphous phase in the range of 20 to 30° (2θ). To gain a deeper understanding of the firing temperature and the different structures among the samples, additional analyses on these samples will be discussed below.

The XRPD results for sample CZT-4006 reveal that this sample is atypical compared to the other samples (this sample is located in groups 1-blue in the PCA plot in Fig. 3). Indeed, the XRPD pattern for this sample exhibits peaks indicating the presence of zeolite mordenite (Fig. 5b). This observation is intriguing because mordenite has been previously associated with the manufacturing of ceramics related to Elamite seals [47, 48]. Mordenite typically occurs with heulandite, and both crystalline phases are typical products resulting from the alteration of volcanic glass fragments [47]. Given the high amorphous content observed in this ceramic body based on the XRPD results, the presence of mordenite may be related to the alteration of the amorphous part.

The samples closest to CZT-4006, as indicated by Figs. 4 and 5a, are CZT-4013 and J-2003, where identifying mordenite peaks is challenging. The XRPD patterns for J-2003 exhibit sharp peaks for calcite, inconsistent with a high firing temperature, as calcite decomposition occurs above 850 °C. SEM–EDXS analysis of the J-2003 sample (Figure S5 and Table S4) revealed zones of altered glassy phases in the ceramic body alongside calcium carbonates. These structures may be related to the firing temperature of the ceramic body, as the amount of glass increases at higher firing temperatures (850–1050 °C), particularly for non-calcareous ceramic bodies [24]. Furthermore, the presence of calcium carbonate in archaeological ceramics is associated with post depositional alteration, and the presence of zeolite may result from the crystallization of minerals left by the alteration of the amorphous phase in overfired ceramics [49]. Therefore, the observation of calcium carbonate and altered glasses in the ceramic body of J-2003 may be attributed to two factors: a high firing temperature and post depositional alteration of the ceramic. Additionally, the aragonite in CZT-4013 likely has a secondary origin, and it was postulated that an organic process may be responsible for its formation [50].

All the samples categorized as quartz-mudstone fabrics according to the petrographic analysis correspond to group 2-red in the PCA plot in Fig. 3, indicating consistent results between the two methods. Additionally, these samples in the SiO_2-Al_2O_3-(CaO + MgO) ternary plot are located in the upper region of the diagram, close to the SiO_2 vertex. Petrographic images reveal incompletely melted quartz grains in these ceramics, with all edges except the center of the quartz grains converted to cristobalite (Fig. 5c). A peak characteristic of cristobalite at $2\theta = 25.6°$ was confirmed in the XRPD patterns (Figure S2). The presence of cristobalite is considered evidence of a prolonged firing time and slow cooling time [51]. In Song Jun Chinese ceramics [52], cristobalite is also observed, and its presence is related to the heat treatment process (long heating and slow cooling). Therefore, the transformation of quartz into cristobalite occurs only after an extended firing time and soaking time. However, during the Elamite period, it is not expected that the kiln temperature can be precisely controlled for a long period. An alternative to prolonged firing or soaking times could be related to the firing conditions. In other words, samples that undergo two rounds of firing (first, firing of the ceramic alone; second, firing when the glaze is added) could exhibit similar characteristics as a prolonged firing and soaking time [53]. Thus, we propose that only during the Neo-Elamite period did artisans experiment with new techniques attempting to fire glazed ceramics twice. This observation is interesting because, as mentioned in the first part of this paper, there are various terms for mudbrick and baked brick during the Elamite period (Table S1). According to the terminology of bricks and glazes during the Elamite period, Potts suggested that some Middle-Elamite bricks were inscribed after glazing but before firing [12]. In other words, in some Elamite

inscribed bricks, the Akkadian term *Libittu* was used, related to mudbrick. However, following this term, they used some colors (silver, gold, blue–green, and white) related to glazes. Therefore, Elamite people applied glaze to mudbrick, not baked- brick, firing both together. Additionally, during the Neo-Elamite period, several new techniques emerged, as indicated by high SiO_2 content in samples from group 2-red.

The four samples included in group 4-Gy (Fig. 3) are identified as calcareous fabrics, specifically those with lime fragments, demonstrating the consistency of results among XRPD, petrographic, and EPMA analyses. Moreover, three samples (HT-1001, HT-1016, and J-2001) within this group are located in an area associated with highly lime-rich samples in Fig. 5a (gehlenite-anorthite-diopside triangle).

According to the petrographic study, the remaining samples, corresponding to group 3-green in the PCA plot (Fig. 3), are void-plant matter fabric and calcareous fabric. Although these fabrics fall under the broader category of calcareous fabrics, the inclusion of plant matter in some samples sets them apart from the rest. As shown in the SiO_2-Al_2O_3-(CaO + MgO) ternary diagram, most of the samples are located in

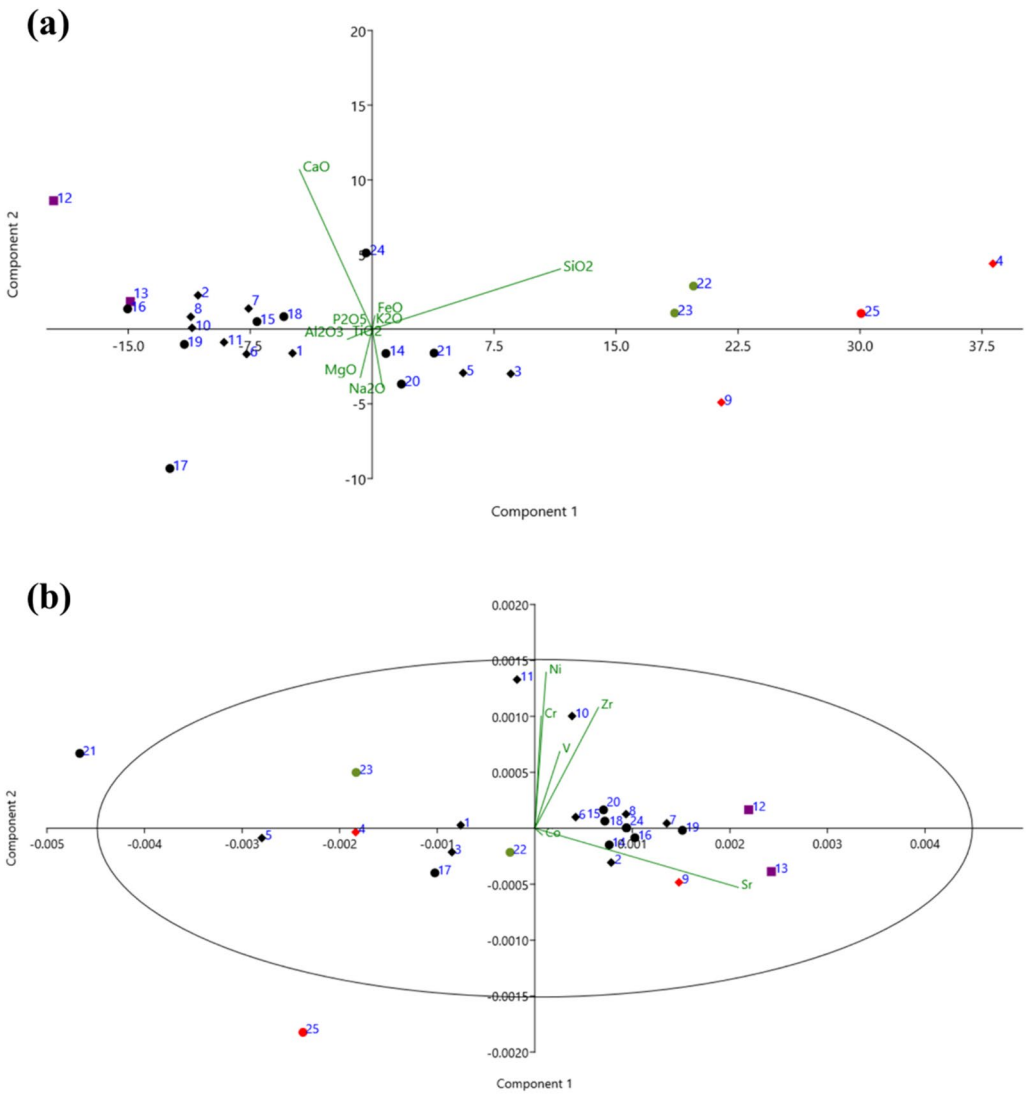

Fig. 6 **a** Bi-plot of PCA (Principal Component Analysis) on the EPMA results of ceramic bodies of Middle-Elamite and Neo-Elamite periods; Square: Haft Tappeh, Losange: Chogha Zanbil, Circle: Jubaji; Red color: Quartz-based ceramic bodies; Olive color: Quartz-Mudstone ceramic bodies; and Purple color represents Calcareous ceramic bodies. **b** Bi-plot of PCA on the trace elements of ceramic bodies of Middle-Elamite and Neo-Elamite periods based on EPMA results with the 95% confidence ellipse. Square: Haft Tappeh, Losange: Chogha Zanbil, Circle: Jubaji; Red color: Quartz-based ceramic bodies; Olive color: Quartz-Mudstone ceramic bodies; and Purple color represents Calcareous ceramic bodies

the quartz-anorthite-diopside triangle, situated away from the quartz-anorthite line. This indicates that these samples can be specifically categorized as calcareous ceramics [53].

Furthermore, considering Fig. 6a, which represents the PCA diagram based on the results of the EPMA analysis, it becomes apparent that pottery samples exhibit more diversity compared to those related to architecture. Specifically, as shown in Fig. 6b, which focuses on the rare elements of ceramic samples, it can be inferred that all samples related to Chogha Zanbil share a common origin, likely produced in proximity to the Chogha Zanbil ziggurat as architecture decorations. However, among Jubaji potteries, there are sherds (samples J-2003 and J-2004) that may have different origins based on their Fig. 6b patterns. Since these types of Jubaji glazed ceramics are all vessel types, the likelihood of their importation is more probable than glazed ceramics from the Middle Elamite period, which are associated with building decorations.

Additionally, among the glazed ceramic samples from Jubaji, only sample J-2003 is considered to have a quartz-based body. Although, from a raw material perspective, according to Fig. 6a, there is not much difference between this sample and the two quartz-based bodies from the Middle-Elamite period (CZT-4006 and CZT-4013), they differ in terms of rare elements. Thus, it can be inferred that the quartz-based ceramic type, which was invented in Khuzestan during the Middle-Elamite period, was likely produced outside of Elam during the Neo-Elamite period and imported into Khuzestan.

Considering that quartz-based glazed bricks have been found abundantly in Persepolis from the Achaemenid period, comparing the structure of Achaemenid quartz-based ceramic bodies with those from the Neo-Elamite period could be interesting in locating the production workshops of these types of ceramics on the Iranian plateau during the sixth and fifth centuries BCE. However, what is now evident is that Khuzestan was probably not the sole center for the production of these types of ceramics on the Iranian plateau by the sixth and fifth centuries BCE.

Another important point, as indicated by Fig. 6a and b, is that the two samples related to Haft Tappeh are slightly separated from the other samples. This suggests that, since the calcium content in these samples is high, it is expected that the strontium content in these samples is also high, given the fact that the strontium content is high in soils with high calcium content. Also, according to Fig. 2b, dolomite has been identified in these two samples, which indicates the difference between these two samples compared to other samples of the Middle Elam and is the reason for the higher calcium content in these two samples. Thus, XRPD analysis of these two samples also suggests the possibility of a difference in the origin of these two samples.

From this perspective, these two samples can also be considered different origin from the other samples. Since the spools found in Susa have been considered as objects from Mesopotamia according to their inscriptions (as a booty) [2], and glazed ceramics are not abundant at Haft Tappeh, it can be assumed that these samples may also have been imported.

Conclusions

A mineralogical and chemical composition study of glazed ceramic bodies from the Middle and Neo-Elamite periods made it possible to examine the samples with a more comprehensive view of ceramic technology, although it should be noted that ceramic bodies often suffer important alterations. For this purpose, XRPD, EPMA, SEM–EDXS, and petrography analyses were performed on the studied samples. The findings revealed that the firing temperature of the pottery falls within the range of 750 to 1000 °C. Convergent results from XRPD, petrography and EPMA allowed us to classify the studied samples into four main groups: siliceous samples, calcareous samples, void-plant matter samples, and quartz-mudstone samples. This classification highlights that two of the four studied groups contain high amounts of quartz. It seems that the ceramic bodies of the Neo-Elamite samples have more diversity compared to those of the Middle-Elamite sample. While the ceramic bodies from the Middle-Elamite period are similar to each other, a greater range of ceramic bodies is observed during the Neo-Elamite period. Notably, two Jubaji samples (J-2009 and J-2002) are different from the others, positioned at the top of the dendrogram. The presence of cristobalite in these two samples suggests differing firing conditions compared to the rest. The variety of ceramic bodies observed during the Neo-Elamite period could be attributed to two factors. Firstly, during this period, there likely existed a wider array of techniques for making and firing ceramic bodies compared to the Middle-Elamite period. Secondly, trade may have also played a role in influencing this diversity. Lastly, the samples classified as quartz based according to petrographic analysis closely resemble the fracture samples in terms of texture. Moreover, these samples exhibit a higher proportion of amorphous compared to others. Given the limited number of samples

in this category, further studies on these glazed ceramic bodies from the Middle- and Neo-Elamite periods are desirable.

Since the pottery associated with vessels all belong to the Neo-Elamite period and after the Assyrian invasion of the land of Elam, they exhibit greater diversity. It is expected that after the extensive Assyrian invasion of the land of Elam, the power of the Elamites in all areas, including the making of glazed pottery, diminished. Therefore, it is likely that some other vessels could not have been produced in the original land of Elam and were imported from other regions into the land of Elam. While during the Middle Elamite period, predominantly glazed artifacts are related to architecture, hence they can generally be considered as made on-site. However, regarding the two spools found at Haft Tappeh, as mentioned earlier, it should also be considered probable that they were imported to the land of Elam.

Supplementary Information

The online version contains supplementary material available at https://doi.org/10.1186/s40494-024-01375-2.

Additional file 1.

Acknowledgements
We would like to thank the following people and museums for their help and assistance: Thierry Pilorge (IRD France) for preparing thin sections. National museum of Iran for collecting the Haft Tappeh and Jubaji glazed ceramics and the Haft Tappeh museum for collecting the Chogha Zanbil glazed ceramics.

Author contributions
Ali Aarab: Methodology, Investigation, Formal analysis, Writing – original draft, Visualization. Laurent Cormier: Conceptualization, Investigation, Project administration, Writing – review & editing, Supervision, Funding acquisition. Bahman Firoozmandi: Conceptualization, Resources, Investigation, Project administration, Writing – review & editing. Martine Gerard: Conceptualization, Resources, Investigation, Project administration, Writing – review & editing.

Funding
This work is supported by the Beijing Natural Science Foundation (IS23041). Also, this research was supported by Région Ile de France grant SESAME 2006 N°I-07–593/R, INSU-CNRS, INP-CNRS, University Pierre et Marie Curie – Paris 6, and by the French National Research Agency (ANR) grant no. ANR-07-BLAN-0124–01.

Availability of data and materials
The datasets generated and analyzed during the current study are available from the corresponding author on reasonable request. Additionally, materials used in this study, such as ceramic samples or analytical tools, are available upon request for research purposes. Data is provided within the manuscript or supplementary information files.

Declarations

Ethics approval and consent to participate
This study does not involve human or animal subjects; hence, ethical approval was not required.

Competing interests
The authors declare no competing interests.

Author details
[1]Department of Archaeology and Anthropology, University of Chinese Academy of Sciences, 100049 Beijing, China. [2]Institut de Minéralogie, de Physique des Matériaux et de Cosmochimie (IMPMC), Sorbonne Université, CNRS UMR 7590, Muséum National d'Histoire Naturelle, IRD UMR 206, 4 Place Jussieu, 75005 Paris, France. [3]Department of Archaeology, Faculty of Literature and Humanities, University of Tehran, 16th Azar Street, Enghlab Avenue, Tehran 1417466191, Iran.

Received: 22 December 2023 Accepted: 16 July 2024
Published online: 02 August 2024

References

1. Negahban EO. Excavations at Haft Tepe, Iran. Philadelphia: University Museum of Archaeology and Anthropology, University of Pennsylvania; 1991.
2. Basello GP. Doorknobs, nails or pegs? The function(s) of the Elamite and Achaemenid inscribed knobs. Persepolis and its settlements: territorial system and ideology in the Achaemenid State. G.P. Basello, A.V. Rossi. Napoli: Università degli studi di Napoli L'Orientale; 2012. p. 1–66.
3. Raith MM, Abdali N, Yule PA. Petrochemical attributes of glazed architectural elements from Middle-Elamite to Achaemenid excavation sites in Iran. Archaeol Anthropol Sci. 2022;14:182.
4. Caubet A, Pierrat-Bonnefois G. Faïences de l'Antiquité: de l'Égypte à l'Iran. Paris: Musée du Louvre éd. 5 Continents; 2005.
5. Caubet A, Bouquillon A, Kaczmarczyk A, Matoïan V, editors. Faïences et matières vitreuses de l'Orient ancien: étude physico-chimique et catalogue des œuvres du département des Antiquités orientales. Paris: Musée du Louvre Éd; 2007.
6. Tite M, Shortland A, Paynter S. The beginnings of vitreous materials in the Near East and Egypt. Acc Chem Res. 2002;35:585–93.
7. Alloteau F, Majérus O, Gerony F, Bouquillon A, Doublet C, Gries H, et al. Microscopic-scale examination of the black and orange-yellow colours of architectural glazes from Aššur, Khorsabad and Babylon in Ancient Mesopotamia. Minerals. 2022;12:311.
8. Shortland AJ, Kirk S, Eremin K, Degryse P, Walton M. The analysis of Late Bronze Age glass from Nuzi and the question of the origin of glass-making. Archaeometry. 2017;60:764–83.
9. Holakooei P. A technological study of the Elamite polychrome glazed bricks at Susa South-Western Iran. Archaeometry. 2014;56:764–83.
10. Emami M, Trettin R. Mineralogical and chemical investigations on the ceramic technology in Čoġā Zanbil, (Iran, 1250 B.C.). Periodico di Mineralogia. 2012;81:359–77.
11. Carter E. Excavations at Anshan (Tal-e Malyan): the Middle Elamite period. Philadelphia: University Museum of Archaeology and Anthropology, University of Pennsylvania; 1996.
12. Potts DT. Elamite temple building. From the foundations to the crenellations: essays on temple building in the Ancient Near East and Hebrew Bible. M.J. Boda, J. Novotny. Münster: Ugarit-Verlag; 2010. p. 49–70.
13. Daucé N. The industry of vitreous materials in Elam. The Elamite world. J. Alvarez-Mon, G.P. Basello, Y. Wicks. London and New-York: Routledge; 2018. p. 568–84.
14. Basello GP, Rossi AV, editors. Persepolis and its settlements: territorial system and ideology in the Achaemenid State. Napoli: Università degli studi di Napoli L'Orientale; 2012.
15. Basello G. Doorknobs, nails or pegs? The function (s) of the Elamite and Achaemenid inscribed knobs. Dariosh Studies II Persepolis and its Settlements: Territorial System and Ideology in the Achaemenid State. 2012;1–66.
16. Shishegar A. Tomb of the Two Elamite Princesses of the House of King Shutur-Nahunte Son of Indada. Tehran: Cultural Heritage, Handcrafts and Tourism Organization; 2015.
17. Ghirshman R. Tchoga Zanbil:(Dur-Untash). 1. La Ziggurat. Geuthner; 1966.
18. Mofidi-Nasrabadi B. Haft Tappeh (Probably Ancient Elamite City of Kabnak). In: Potts DT,Harkness E, Neelis J, McIntosh RJ, editors. The Encyclopedia of Ancient History [Internet]. 1st ed. Wiley; 2021 [cited 2024 Jul 4]. p. 1–7. https://onlinelibrary.wiley.com/doi/https://doi.org/10.1002/9781119399919.eahaa00036

19. Ahmadinia R, Shishegar A. Jubaji, a Neo-Elamite (Phase IIIB, 585–539 BC) Tomb in Ramhurmuz. Khuzestan Iran. 2019;57:142–74.
20. Ghirshman R. The ziggurat of Tchoga-Zanbil. Sci Am. 1961;204:68–77.
21. Holakooei P. Technological study of the seventeenth century haft rang tiles in Iran with a comparative view to the cuerda seca tiles in Spain. Le migliori tesi. 2016;8:1–147.
22. Whitbread IK. The characterisation of argillaceous inclusions in ceramic thin sections. Archaeometry. 1986;28:79–88.
23. Quinn PS. Ceramic petrography: The interpretation of archaeological pottery & related artefacts in thin section. Oxford: Archaeopress Publishing Ltd; 2013.
24. Maniatis Y, Tite MS. Technological examination of Neolithic-Bronze Age pottery from central and southeast Europe and from the Near East. J Archaeol Sci. 1981;8:59–76.
25. Freestone IC, Middleton AP. Mineralogical applications of the analytical SEM in archaeology. Mineral Mag. 1987;51:21–31.
26. Heydarian M, Abdorrahimian F, Emami SMA, Beheshti SI. The provenance and distribution of early Bronze ceramics in the Kolyaei Plain, central Zagros. Iran Archaeometry. 2020;62:694–711.
27. Papachristodoulou C, Oikonomou A, Ioannides K, Gravani K. An X-Ray fluorescence and principal component analysis study of pottery from Orraon. HNPS Adv Nucl Phys. 2019;14:107–12.
28. Bajnok K, Kovács Z, Gait J, Maróti B, Csippán P, Harsányi I, et al. Integrated petrographic and geochemical analysis of the Langobard age pottery of Szólád Western Hungary. Archaeol Anthropol Sci. 2022;14:13.
29. Fügert A, Gries H. 'I had baked bricks glazed in lapis lazuli color'1 – A brief history of glazed bricks in the ancient Near East. Glazed Brick Decoration in the Ancient Near East. A. Fügert, H. Gries. Oxford: Archaeopress Archaeology; 2020. p. 1–15.
30. Roach KJ. The Elamite cylinder seal corpus, c.3500 – 1000 BC [PhD Thesis]. [Sidney]: University of Sidney; 2008.
31. Travé AE. Colour transformation and textural change in biotite: Some remarks for the interpretation of firing technology in greyware pottery thin-sections. Minerals. 2021;11:428.
32. Fronteau G, van den Bel M. Anthropogenic temper *versus* geological and pedological inclusions: grog temper as a possible chrono-cultural marker for the Late Ceramic Age in the pre-Columbian Lesser Antilles. BSGF - Earth Sci Bull. 2021;192:17.
33. Fabbri B, Gualtieri S, Shoval S. The presence of calcite in archeological ceramics. J Eur Ceram Soc. 2014;34:1899–911.
34. Rathossi C, Pontikes Y, Tsolis-Katagas P. Mineralogical differences between ancient sherd and experimental ceramics: indices for firing conditions and post-burial alteration. Bull Geol Soc Greece. 2017;43:856–68.
35. Wiśniewska K, Kłosek-Wawrzyn E, Lach R, Pichór W. Influence of the grain size distribution of the limestone additives on the color properties and phase composition of sintered ceramic materials based on cream-firing clays. Materials. 2022;15:2694.
36. Emami M, Emami SN. A time-dependent statistical evaluation of the ceramic manufacturing process based on the mineralogical chemical analysis. ArchéoSciences. 2020;1:145–59.
37. Noll W, Heimann RB. Ancient old world pottery: materials, technology, and decoration. Stuttgart: Schweizerbart Science Publishers; 2016.
38. Gorres M, Evangelakakis C, Kroll H. Mineralogical technologies in archeology: Their application to grey-Minyan ceramics of Troy VI. In: Dirksen D, Von Bally G, editors. Optical Technologies in the Humanities [Internet]. Berlin, Heidelberg: Springer Berlin Heidelberg; 1997. p. 134–6. Available from: http://link.springer.com/https://doi.org/10.1007/978-3-642-60872-8_16
39. Moroni B, Conti C. Technological features of Renaissance pottery from Deruta (Umbria, Italy): an experimental study. Appl Clay Sci. 2006;33:230–46.
40. Cultrone G, Rodriguez-Navarro C, Sebastian E, Cazalla O, De La Torre MJ. Carbonate and silicate phase reactions during ceramic firing. Eur J Mineral. 2001;13:621–34.
41. Rösch C, Hock R, Schüssler U, Yule P, Hannibal A. Electron microprobe analysis and X-ray diffraction methods in archaeometry: Investigations on ancient beads from the Sultanate of Oman and from Sri Lanka. Eur J Mineral. 1997;9:763–83.
42. Rathossi C, Pontikes Y. Effect of firing temperature and atmosphere on ceramics made of NW Peloponnese clay sediments Part I: Reaction paths, crystalline phases, microstructure and colour. J Eur Cer Soc. 2010;30:1841–51.
43. Javanshah Z. Chemical and mineralogical analysis for provenaning of the Bronze Age pottery from Shahr-I-Sokhta. South Eastern Iran. 2017;4:83–92.
44. Portilla-Mendoza KA, Pinzón-Núñez DA, Moreno-González L, Mier-Umaña R, Ríos-Reyes CA, Henao-Martínez JA. Mineralogical characterization of pre-hispanic pottery at the Mesa de Los Santos region. Colombia Boletín de Geología. 2019;41:123–36.
45. Grammatikakis IE, Kyriakidis E, Demadis KD, Diaz AC, Leon-Reina L. Mineralogical characterization and firing temperature delineation on Minoan pottery, focusing on the application of micro-Raman spectroscopy. Heritage. 2019;2:2652–64.
46. Sedghi Y, Sani FS, Eskandari N, Emami M. Beyond a decoration; Mineralogical and micro-structural study of the early Bronze Age "Life Cycle Jar" from Keshik cemetery, Sistan and Balouchistan Iran. Interdisciplinaria Archaeologica Nat Sci Archaeol. 2022;13:117–28.
47. Sax M, Middleton AP. The use of volcanic tuff as a raw material for proto-Elamite cylinder seals. Iran. 1989;27:121.
48. Lahanier C. Note sur l'emploi de l'heulandite et de la mordénite dans la fabrication de sceaux cylindres proto-élamites. 1976;Annales du Laboratoire de Recherche des Musées de France:65–6.
49. Gilstrap WD, Meanwell JL, Paris EH, López Bravo R, Day PM. Post-depositional alteration of calcium carbonate phases in archaeological ceramics: depletion and redistribution effects. Minerals. 2021;11:749.
50. Oudbashi O, Naseri R, Cultrone G, Egartner I, Arizzi A. The pottery production from the Deh Dumen Bronze Age graveyard (South-Western Iran): a chemical, mineralogical and physical study. Heritage Science. 2021;9:83.
51. Reedy CL. Petrographic and image analysis of thin sections of classic wares of Song dynasty. Proceedings of International Symposium on Science and Technology of Five Great Wares of the Song Dynasty. Shi Ningchang and Miao Jianmin. Beijing: Science Press.
52. Yang M-L, Katz JI, Barton J, Lai W-L, Jean J-H. Using optical coherence tomography to examine additives in Chinese Song Jun glaze. Archaeometry. 2015;57:837–55.
53. Holakooei P, Tessari U, Verde M, Vaccaro C. A new look at XRD patterns of archaeological ceramic bodies: an assessment for the firing temperature of 17th century haft rang tiles from Iran. J Therm Anal Calorim. 2014;118:165–76.

Publisher's Note